Catalysis Science & Technology

Accepted Manuscript

ROYAL SOCIETY OF CHEMISTRY

www.rsc.org/catalysis

Direct synthesis of hydrogen peroxide from hydrogen and oxygen over activated-carbon-supported Pd-Ag alloy catalysts

Junjie Gu, Suli Wang, Zhiyuan He, You Han, Jinli Zhang *

School of Chemical Engineering and Technology, Tianjin University,

Tianjin 300072, China

* Corresponding Author: Tel: +86-22-27401476; Fax: +86-22-27403389

E-mail: zhangjinli@tju.edu.cn

Abstract

A series of bimetallic PdAg catalysts with the support of activated carbon were prepared and assessed for the direct synthesis of hydrogen peroxide from hydrogen and oxygen. The ensemble effect and electronic effect between Pd and Ag were characterized including X-ray diffraction (XRD), X-Ray photoelectron spectroscopy (XPS), temperature-programmed reduction (TPR), and temperature-programmed desorption of H_2/O_2 (H_2-/O_2-TPD), etc. Our results showed that the Ag additive increased the monomer Pd sites which were the primary active sites for H_2O_2 formation. In addition, the content of Pd^{2+} was increased via the electronic interaction between Pd and Ag, which prevented the decomposition and hydrogenation of H_2O_2 to some extent. Therefore, the selectivity of this reaction was increased via using bimetallic PdAg catalysts compared with the monometallic Pd catalyst. The optimal PdAg-40 catalyst achieved a H_2O_2 productivity of 7022mol kg_{Pd}^{-1} h^{-1} and a high selectivity of 70.9%, which were superior to those of the Pd/C catalyst.

Keywords: PdAg alloy, direct synthesis of hydrogen peroxide, ensemble effect,

electronic effect

1. Introduction

Hydrogen peroxide (H_2O_2) is recognized as an environmental friendly oxidizing agent widely used in industry, such as in the industry of electron, chemical synthesis, pharmaceutical, papermaking, waste water treatment and so on.[1-5] By far the main industrial production of H_2O_2 is an indirect process involving sequential hydrogenation and oxidation of an anthraquinone precursor, which consumes energy intensively requiring the periodic replacement of anthraquinone due to excessive hydrogenation.[6-9] The direct synthesis of H_2O_2 from H_2 and O_2 is promising to be a viable candidate to produce H_2O_2 industrially for its remarkable advantages of atom economy, less energy consumption, and low operating costs.[10]

Pd supported catalysts have been widely applied in the direct synthesis reaction.[11-19] The major problem associated with the direct synthesis of H_2O_2 is the low H_2O_2 selectivity, since Pd is also very active for the formation of H_2O, H_2O_2 decomposition and hydrogenation. Continuous efforts have been made to control the catalytic performance of Pd by incorporating other metals into the Pd catalysts.[20-40] Hutchings et al. reported that the addition of Au into Pd catalyst led to a substantial improvement in both the overall activity and the H_2O_2 selectivity.[20-31] For a 2.5 wt% Pd-2.5 wt% Au/C catalyst, a H_2O_2 productivity of 110 mol kg_{cat}^{-1} h^{-1} and a H_2O_2 selectivity of 80% were obtained, which were much higher than those of the pure 5.0 wt% Pd with a H_2O_2 productivity of 55 mol kg_{cat}^{-1} h^{-1} and a H_2O_2 selectivity of 34%. Similar phenomena were also observed for the TiO_2-supported and Al_2O_3-supported

Pd-Au catalysts.[22] The reports demonstrated that the synthesis and hydrogenation of H_2O_2 operated at the same active sites for mono Pd catalysts, while the Pd-Au bimetallic catalysts had different active sites.[31] Ouyang et al.[36] studied the active sites of Pd-Au alloy catalysts in the direct synthesis of H_2O_2, concluding that Au increased the mono-Pd sites while reduced the contiguous Pd sites. The mono Pd atoms surrounded by Au atoms were assumed to be more favorable for H_2O_2 formation, while contiguous Pd ensembles were more favorable for H_2O_2 hydrogenation. Pd-Pt bimetallic catalyst was another potential candidate for the direct synthesis of H_2O_2.[37-40] Bernardotto et al. [38] reported that a low Pt content (0.1 wt%) in Pd catalyst could improve H_2O_2 selectivity (from 55% to 68%) and productivity (from 915 to 1083 mmol g_{metal}^{-1} h^{-1}) with respect to the 1.0 wt% Pd. Han et al.[39] also reported that $Pd_{16}Pt_1$ (3.3 wt% Pd, molar ratio Pd/Pt=16) exhibited a H_2O_2 productivity of 1770 mol kg_{Pd}^{-1} h^{-1} and a selectivity of 60%, while 990 mol kg_{Pd}^{-1} h^{-1} and 12% were observed for pure Pd. They speculated that the Pt additive assisted Pd in stabilizing dioxygen by modifying the electronic structure of Pd. According to these previous reports, the improved catalytic performance of Pd-based catalysts incorporated with other metals for the direct synthesis of H_2O_2 was attributed to ensemble effect and electronic effect between metals.

Noticeably, the additives Au and Pt described in the literature are very expensive. One way of reducing their consumption is to replace some costly noble metals by introducing some non-noble metals. Bimetallic Pd-Ag systems have displayed outstanding performance for some important reactions such as selective

hydrogenation of acetylene,[41-50] selective oxidation of glycerol to dihydroxyacetone,[51, 52] hydrogenation of alkynol[53] and etc. Both ensemble effect and electronic effect were detected in these Pd-Ag particles. The ensemble effect was caused by that Ag reduced the number of neighbored Pd-atoms, forming Pd-islands and single Pd-surface atoms.[47-51, 54] The electronic properties of Pd were modified by Ag and the charge transfer between Pd and Ag was found by some researchers.[41, 42, 50] However, to our best knowledge, no report has been found on the performance of bimetallic Pd-Ag catalysts for the direct synthesis of H_2O_2 from H_2 and O_2.

Previously, Pd-Ag alloy membranes were prepared using electroless plating techniques and studied for the direct synthesis of H_2O_2 from H_2 and O_2. For example, Abate et al.[55, 56] reported that Pd-Ag alloy could improve the stability of the Pd-Ag membrane by limiting the formation of β-PdH in the presence of H_2 diffusing through the membrane, which usually caused the brittleness of the Pd film. Wang et al. [57] reported that H_2O_2 could be formed from H_2 and O_2 with a fair productivity using the Pd-Ag alloy membrane with the inside layer of Pd-Ag and the outside layer of active Pd. However, these reports did not study the effect of Ag on the catalytic performance of Pd catalysts. Recently, Farberow et al.[58] demonstrated that Ag(111) was more selective toward H_2O_2 than Pd(111), as Ag(111) was more effective at suppressing O-O bond scission through first principles electronic structure calculations. Hence, we are inspired to investigate whether or not the bimetallic Pd-Ag catalysts show high activity toward the direct synthesis of H_2O_2 from hydrogen and oxygen as well as the side reactions in the system, in order to explore a promising catalyst for the direct

synthesis of H_2O_2.

In this article, for the first time we prepared a series of bimetallic PdAg catalysts and investigated extensively the performance these supported PdAg catalysts for the direct synthesis of H_2O_2 in a slurry reactor. The modification of the Pd surface upon alloying with Ag and the electron transfer between the metals were connected with the catalytic properties of supported Pd-Ag systems after detailed characterization using X-ray diffraction (XRD), X-Ray photoelectron spectroscopy (XPS), temperature-programmed reduction (TPR), and temperature-programmed desorption of H_2/O_2 (H_2-/O_2-TPD), etc.

2. Experimental

2.1 Catalyst preparation

PdAg/C catalysts were prepared by the conventional incipient wetness impregnation method. $Pd(NO_3)_2$ (AR, Tianjin Guangfu Fine Chemical Research Institute) solution was used as the Pd precursor and $AgNO_3$ (AR, Tianjin Guangfu Fine Chemical Research Institute) as the Ag precursor. Activated carbon (200-400 mesh) was used as the support. A slurry of activated carbon in a $Pd(NO_3)_2$ and $AgNO_3$ aqueous solution was stirred at 45 ^oC for 1 h. Then the impregnated samples were filtered, washed with deionized water, dried at 120 ^oC overnight and finally calcined in static air at 300 ^oC for 4 h. The loading amount of Pd was fixed at 1 wt%. Four catalysts samples were prepared with Pd/Ag molar ratios of 60:1, 40:1, 20:1 and 10:1, which were named as PdAg-60, PdAg-40, PdAg-20, and PdAg-10, respectively. For comparison, mono Pd and mono Ag catalysts with metal content of 1 wt% were

prepared using the same procedures.

2.2 Catalytic performance test

2.2.1 Direct synthesis of H_2O_2

Prior to the reaction, the samples were pretreated at 500 ^oC in 10% H_2/Ar for 4 h. The catalysts were evaluated for the direct synthesis of H_2O_2 in a stainless steel autoclave coated with Teflon. The autoclave was equipped with a magnetic stirrer and made provision for measuring temperature and pressure. Typically, 0.2 g catalyst and 20 ml of a 0.03 M H_2SO_4 methanolic solution were put into the reactor. The reactor was purged three times with N_2 (3 MPa) and then filled with 5% H_2/N_2 and 25% O_2/N_2 to give a H_2-to-O_2 ratio of 1:2 at a total pressure of 3 MPa at 2 ^oC. After reacting for 15 min, the suspension was separated by centrifugal. H_2O_2 content $n(H_2O_2)$ was measured by titration with acidified $Ce(SO_4)_2$, and water content $n(H_2O)$ was determined by volumetric Karl–Fischer method. The productivity is defined as the moles of H_2O_2 produced per kilogram of Pd per hour. H_2 conversion and H_2O_2 selectivity were calculated according to the following equations.

$$Conversion = \frac{n(H_2O_2) + n(H_2O)}{n(H_2)} \times 100\% \quad (1)$$

$$Selectivity = \frac{n(H_2O_2)}{n(H_2O) + n(H_2O_2)} \times 100\% \quad (2)$$

2.2.2 Hydrogenation and decomposition of H_2O_2

The hydrogenation and decomposition of the H_2O_2 reactions were analogous to those of direct synthesis but introducing a H_2SO_4 methanolic solution containing 1 wt% H_2O_2. Hydrogenation experiments were carried out in the atmosphere of 5% H_2/N_2

while decomposition reactions only using a gas feed of pure N_2. The H_2O_2 conversion rate is defined as the moles of H_2O_2 consumed per kilogram of Pd per hour.

2.3 Catalyst characterization

N_2 adsorption-desorption isotherms were measured on a Micromeritics ASAP 2020 instrument at -196 ^oC. Inductively coupled plasma-atomic emission spectrometry (ICP-AES) was carried out using an Iris advantage Thermo Jarrel Ash device. XRD patterns were measured from 10 to 90^o 2θ using a Bruker D8 Advance diffractometer equipped with a Si (Li) solid-state detector (SOL-X) and a sealed tube providing Cu Kα radiation. Transmission electron microscopy (TEM) analysis was carried out using a JEOL JEM2010 microscope under an accelerating voltage of 200 kV. XPS was recorded using a Kratos Axis Ultra DLD spectrometer employing a monochromated Al-Kα X-ray source (hν=1486.6 eV), hybrid (magnetic/electrostatic) optics, a multi-channel plate and delay-line detector (DLD). All the binding energies were referenced to the C_{1S} peak at 284.6 eV. TPR experiments were performed with a AutoChem BET TPR/TPD (Quantachrome Instruments AMI-90) connected to a thermal conductivity detector (TCD): a sample of 100 mg was heated from room temperature to 600 ℃ at a heating rate of 10 ℃ min^{-1} under a flow of 10% H_2/Ar. H_2-/O_2-TPD experiments were also performed with a AutoChem BET TPR/TPD (Quantachrome Instruments AMI-90) connected to a thermal conductivity detector (TCD). Prior to the absorption, the catalyst was reduced in 10% H_2/Ar at 500 ℃ for 60 min, then cooled down in pure He. Absorbents of 10% H_2/Ar or 10% O_2/Ar were introduced into the system at 40 ℃ for 15 min. Afterwards, the system was purged

with He for 15 min. The temperature was ramped from 40 ℃ to 500 ℃ with a rate of 10 ℃ min^{-1} in He.

The N_2 adsorption-desorption, ICP, H_2-TPR, H_2-TPD and O_2-TPD investigations were performed with fresh catalysts and the XRD, TEM and XPS investigations were performed using the reduced catalysts.

3. Results

3.1 Catalyst characterization

3.1.1 Catalyst textural properties and chemical compositions

The textural properties and compositions of the catalysts are summarized in Table 1. The activated carbon exhibited microporous structure with S_{BET}=1181 m^2 g^{-1}, V_p=0.57 cm^3 g^{-1}, D_p=1.92 nm. After loading with the metallic components, both the surface area and the total pore volume were reduced, which was attributed to the pore blockage caused by metallic components during the catalyst preparation.

The Pd and Ag amounts of the final samples were analyzed by ICP. As can be observed in Table 1, the measured amounts of Pd and Ag were lower than the theoretical values, which was due to incomplete adsorption of metal ions on the support. The actual molar ratios in the bimetallic catalysts were 73:1, 46:1, 24:1, and 12:1, which were close to the nominal value 60:1, 40:1, 20:1, and 10:1, respectively.

Table 1 Chemical compositions and textural properties of the calcined catalysts and bare support.

Sample	Pd (wt%)[a]	Ag (wt%)[a]	S_{BET} (m^2 g^{-1})[b]	Vp (cm^3 g^{-1})[b]	D_p (nm)[b]
carbon	--	--	1181	0.57	1.92
Pd	0.96	0	1126	0.54	1.92
PdAg-60	0.88	0.012	1134	0.55	1.93
PdAg-40	0.83	0.018	1126	0.54	1.93
PdAg-20	0.86	0.036	1130	0.55	1.93
PdAg-10	0.86	0.070	1132	0.55	1.93
Ag	0	0.673	1138	0.55	1.93

[a] As determined by ICP.

[b] BET surface area, total pore volume (V_p) and average pore diameter (D_p) were measured from the N_2 adsorption-desorption isotherms.

3.1.2 TEM

TEM images obtained for the Pd/C, Ag/C and bimetallic PdAg/C catalysts, as well as the particle size distribution histograms are represented in Fig. 1. The average particle size of Pd/C and Ag/C was estimated to be 15.8 and 18.8 nm, respectively. The formation of larger Ag particles could be attributed to a weaker interaction between the Ag particles and the support.[59] The average particle size decreased to 14.3 nm (PdAg-60) after a small addition of Ag, achieving the smallest size (12.3 nm) at the Pd/Ag molar ratio of 20:1. However, the growth in particle size could be observed with further increasing the Ag content. The average size of PdAg-10 was 14.5 nm. Thus, the addition of moderate Ag was beneficial to disperse the active components on the activated carbon support surface.

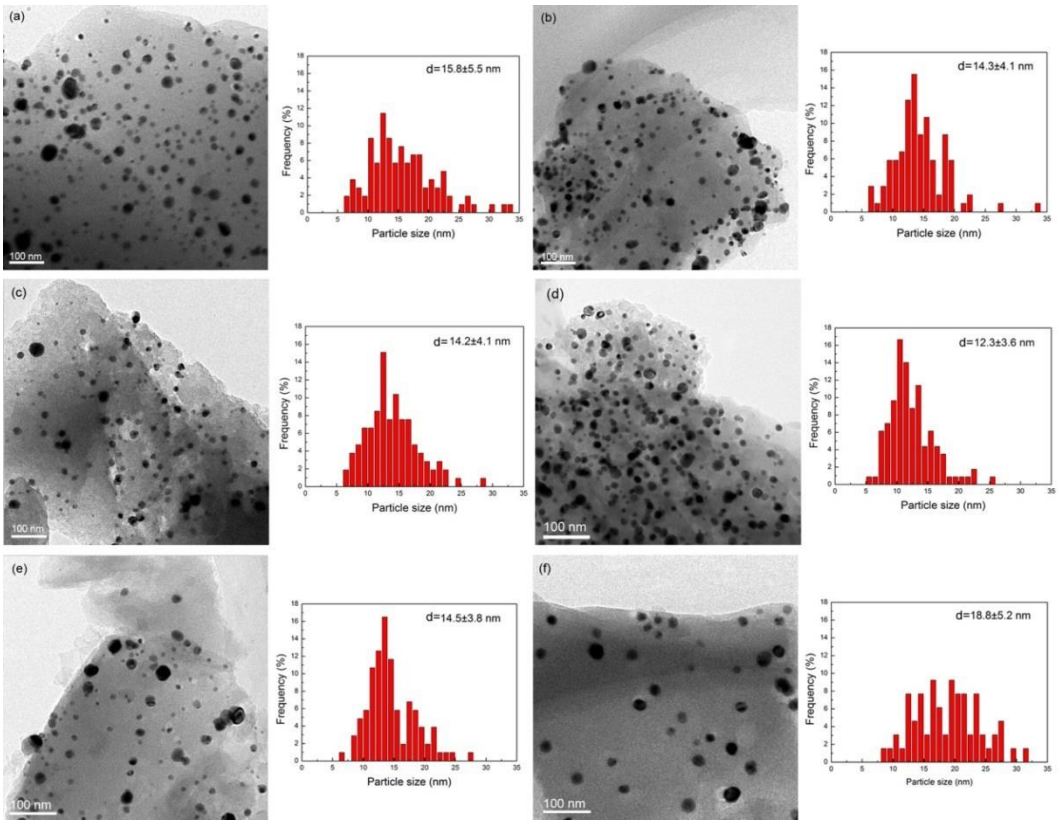

Fig. 1 TEM images of the fresh reduced catalysts: (a) Pd, (b) PdAg-60, (c) PdAg-40, (d) PdAg-20, (e) PdAg-10, (f) Ag.

3.1.3 XRD

The metal crystallites of the catalysts were characterized using XRD and the results are shown in Fig. 2(a). All of the samples exhibited four clear diffraction peaks, indexed as the (1 1 1), (2 0 0), (2 2 0) and (3 1 1) planes of a face-centered cubic structure.[60] The peak observed at 23.8^{o} was the characteristic peak of activated carbon.[61, 62] No characteristic diffraction peaks of Ag were observed in all PdAg catalysts. This phenomenon indicated that Ag has entered into the Pd crystal lattice and formed a solid solution with Pd or probably because the Ag in PdAg catalysts was only present in low amount. Compared with mono Pd catalysts, the four diffraction peaks of Pd in the PdAg catalysts slightly shifted to a lower scanning angle. As shown in Fig. 2(b), it can be clearly observed from the enlarged regional pattern between 43^{o}

and 48° that (200) plane peaks of Pd shifted ca. 0.02-0.32° toward lower scanning angle for the Pd-Ag catalysts compared with the Pd/C. These results indicated that Ag has entered into the Pd crystal lattice forming PdAg alloys.[60, 63]

The molar compositions of Pd and Ag in the alloys were obtained by using Vegard's law, the (2 0 0) peak was used to analyze the lattice constant. As shown in Table 3, the atomic fractions of Ag in the PdAg alloys were very close to the ICP results, implying that almost all Ag atoms have entered into Pd crystal lattice to form PdAg alloys.[62]

Scherrer's equation was used to estimate the particle size of the metal nanoparticles and the results are listed in Table 2. The particle size decreased from 12.7 (Pd/C) to 11.4 nm (PdAg-20) with the addition of Ag, inversely with further increasing the amount of Ag. This result was in accordance with size observed by TEM. Because the average pore diameter of the bare support was about 1.9 nm, these particles could not enter into the activated carbon pores and were located on the external surface.

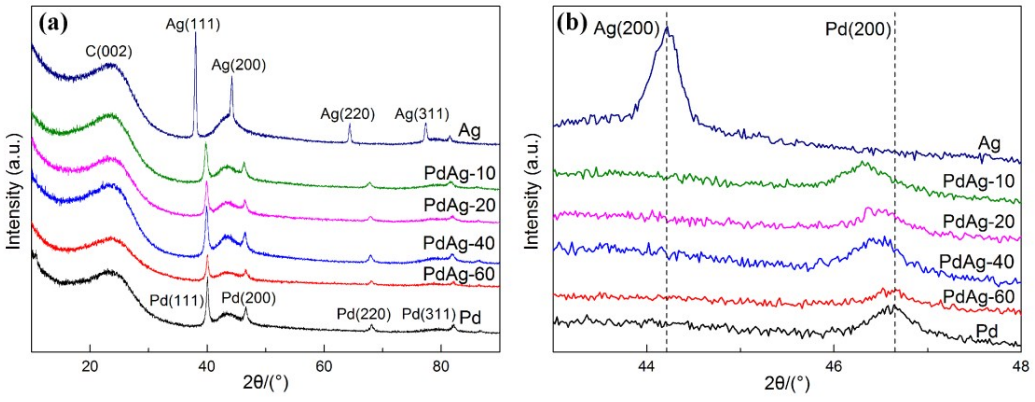

Fig. 2 (a) XRD patterns of Pd, PdAg-60, PdAg-40, PdAg-20, PdAg-10, and Ag catalysts; (b) enlarged regional pattern between 43° and 48° over all catalysts.

Table 2 Particle sizes of the catalysts.

Catalysts	*d* (nm) from TEM	*d* (nm) from XRD
Pd	15.8	12.7
PdAg-60	14.3	12.2
PdAg-40	14.2	11.6
PdAg-20	12.3	11.4
PdAg-10	14.5	13.8
Ag	18.8	17.2

3.1.4 TPR

To further understand the interaction between Pd and Ag, the reducibility of the unreduced samples was investigated by H_2-TPR, and the results are shown in Fig. 3. For the Ag/C catalyst, there weren't any reduction peaks of Ag were observed, which was because that Ag_2O decomposed to Ag during the calcination process. [64] The Pd/C catalyst presented H_2 consumption peaks at 47 and 368 ^oC, which were due to the reduction of surface PdO and subsurface PdO, respectively.[63, 65] The reverse peak observed at 101 ^oC was caused by H_2 decomposition of Pd β-hydride.[66, 67] For all the PdAg/C samples, the two reduction peaks of PdO shifted to higher temperature, indicating that Ag makes PdO less likely to be reduced, a suggestion supported by the XPS results showing that the fraction of Pd^{2+} increased with the addition of Ag. It should also be noted that the intensity of the H_2 desorption peak decreased and the position shifted towards higher temperature with the increase of Ag amount, suggesting that Ag inhibited the formation of Pd β-hydride. This phenomenon indicated the presence of mixed bimetallic system[66] which was also detected by our XRD measurement. Considering that the reducibility of the metal catalyst is related to the electronic structure of the metal,[68] we suggested that Ag has modified the electronic properties of Pd.

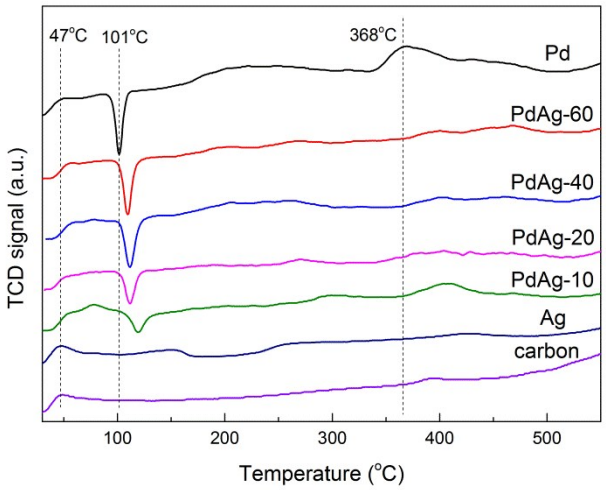

Fig. 3 H_2-TPR profiles of carbon support and Pd, PdAg-60, PdAg-40, PdAg-20, PdAg-10, Ag catalysts.

3.1.5 XPS

XPS was performed to analyze the surface compositions, chemical states and the electronic interactions between Pd and Ag of the different catalysts. The Pd*3d* and Ag*3d* spectra of the catalysts are listed in Fig. 4. A shift of ca. 0.1-0.3 eV towards high binding energy with respect to the mono Pd was detected in the bimetallic PdAg catalysts. Whereas the Ag peaks shifted ca. 0.6-1.0 eV toward low binding energy with respect to the mono Ag. These results implied that the electronic structure of the surface Pd atoms was modified upon the addition of Ag. That is, the Pd species in the PdAg samples was electron deficient, which could be attributed to the charge transfer from Pd to Ag.[41, 69, 70]

The XPS-derived atomic ratio Pd^{2+}/Pd was analyzed using the peak-fitting method. As listed in Table 3, the percentage of Pd^{2+} elevated with the amount of Ag increased, implying the Pd species acted as electronic supplier for Ag.

The atomic percentages of Ag on the surface or in the bulk phase of PdAg

catalysts were also calculated. As listed in Table 3, the atomic percentages of Ag on the surface of PdAg alloys were obviously greater than those in bulk phase determined by ICP and XRD, suggesting that Ag was rich in the surface. The surface enrichment of Ag in PdAg bimetallic catalysts was due to the low surface energy of Ag with respect to Pd.[71, 72]

Table 3 Ag atom percent in metal-phase and the surface Pd^{2+} percent of the catalysts.

Catalysts	Bulk Ag atom percent (%) [a]	Alloy Ag atom percent (%) [b]	Surface Ag atom percent (%) [c]	Pd^{2+} (%) [c]
Pd	--	--	--	34.2
PdAg-60	1.3	1.4	6.1	34.9
PdAg-40	2.1	2.3	7.8	38.5
PdAg-20	4.0	4.8	19.1	39.4
PdAg-10	7.7	9.6	20.0	40.8
Ag	--	--	--	--

[a] From ICP. [b] From XRD. [c] From XPS.

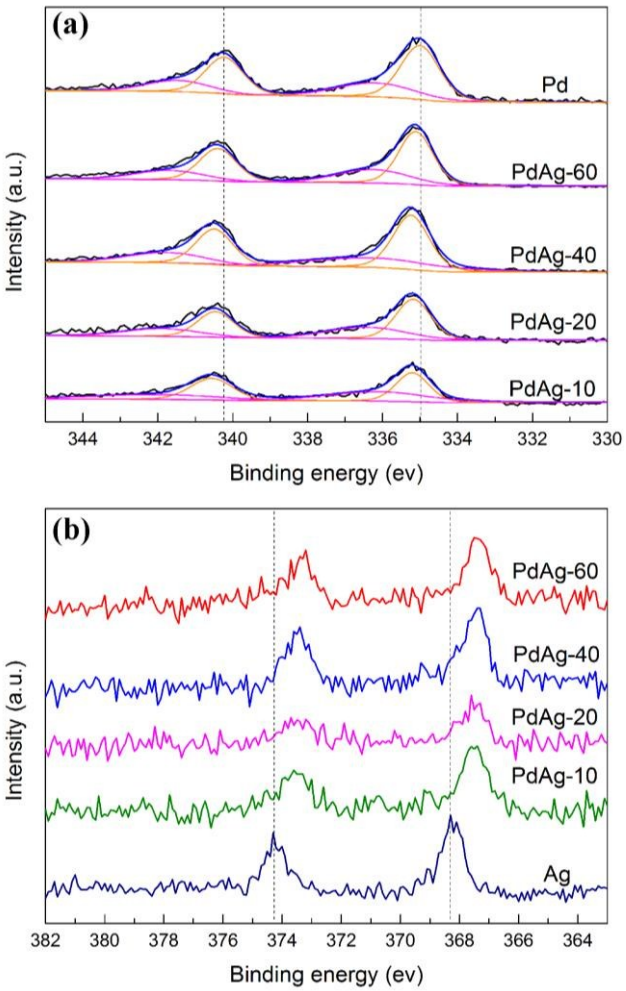

Fig. 4 (a) XPS Pd3*d* spectroscopy and (b) XPS Ag3*d* spectroscopy over the reduced catalysts.

3.1.6 O_2-TPD and H_2-TPD

The O_2-TPD profiles recorded for all catalysts are listed in Fig. 5. For the Ag/C, the profile was a straight line without any O_2 desorption peak, indicating that Ag is lack of affinity towards O_2 due to its filled *d*-band. The O_2 desorption peak was detected at 366 ^{o}C for Pd/C. For the bimetallic PdAg catalysts, the desorption temperature gradually decreased to 343 ^{o}C with the decrease of Pd/Ag ratio, indicating the presence of Ag weakened the interaction between O_2 and Pd. Meanwhile, a decrease in the desorption amount of O_2 from 14.6 (Pd) to 6.3 mmol g_{Pd}^{-1} (PdAg-10) (Table 4) indicated PdAg alloys had less O_2 adsorption sites than mono Pd.

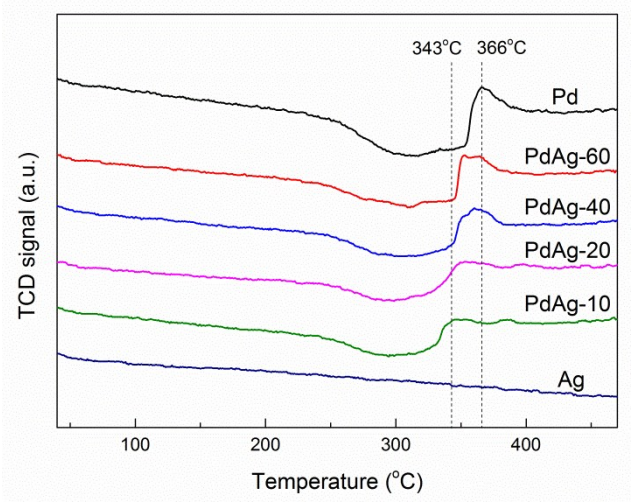

Fig. 5 O_2-TPD profiles obtained for different catalysts.

H_2-TPD experiments were also performed and the results are given in Fig. 6. The desorption peak at 171 °C was derived from H_2 chemisorption on the Pd surface sites, whereas there had no adsorption between H_2 and Ag.[73-75] As observed in Table 4, the desorption amount of H_2 decreased steadily from 78.0 (Pd) to 43.6 mmol g_{Pd}^{-1} (PdAg-10) with a continuous increase in the Ag concentration, showing Ag reduced the H_2 adsorption ability of Pd.

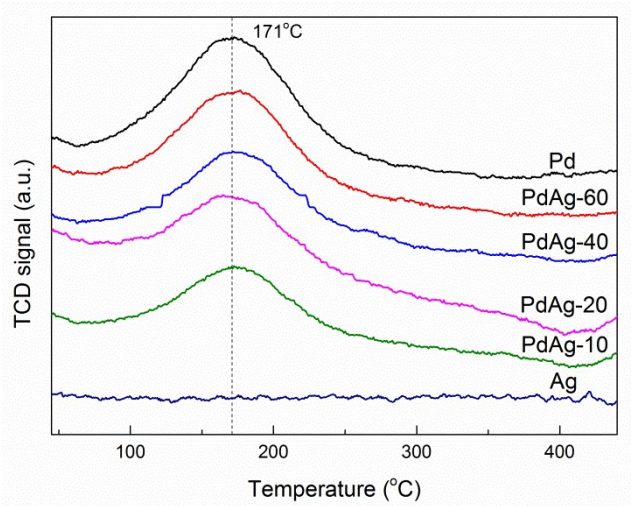

Fig. 6 H_2-TPD profiles obtained for different catalysts.

Table 4 The absorption amount of H_2 and O_2 over all catalysts.

Catalysts	Desorption amount of O_2 ($\mu mol\ g_{Pd}^{-1}$)	Desorption amount of H_2 ($\mu mol\ g_{Pd}^{-1}$)
Pd	771	3867
PdAg-60	661	3127
PdAg-40	616	2579
PdAg-20	421	2291
PdAg-10	331	2126
Ag	0	0

3.2 Catalytic behavior

3.2.1 H_2O_2 direct synthesis

All the synthesis experiments were carried out for three times to ensure the accuracy of test. The catalytic performances of all the catalysts are summarized in Table 5. Neither H_2O_2 nor H_2O was obtained for Ag/C under the given condition, implying Ag was inactive for this reaction. The Pd/C catalyst showed a H_2 conversion of 93.6% and a H_2O_2 selectivity of 54.0%. The catalyst performance was significantly changed upon alloying with Ag. The H_2 conversion decreased steadily with a continuous increase in the Ag concentration. The conversion of the PdAg-10 (28.1%) was much lower than mono-Pd (93.6%). However, the selectivity of the Pd catalysts could be enhanced by the addition of Ag. It could be observed that just very little amount of Ag, such as PdAg-60 (0.012 wt%), could enhanced H_2O_2 selectivity to 63.5% and it continued to increase to 70.9% for PdAg-40 (0.018 wt%), these results were in coincidence with the previous prediction by Farberow et al.[58] Further increasing Ag content resulted in a very small increment of H_2O_2 selectivity and finally it remained at about 72%. The H_2O_2 productivity was affected both by the H_2 conversion and H_2O_2 selectivity. The PdAg-40 achieved the highest H_2O_2 productivity of 7022 mol

kg_{Pd}^{-1} h^{-1}, which was 9.8% higher than that of the Pd/C catalyst.

Table 5 The performance of all the catalysts in the H_2O_2 synthesis directly from H_2 and O_2.

catalysts	Conversion (%)[a]	Selectivity (%)[a]	Productivity (mol kg_{Pd}^{-1} h^{-1})[a]
Pd	93.6±2.1	54.0±0.7	6397±243
PdAg-60	76.1±3.0	63.5±1.0	6674±147
PdAg-40	67.6±1.8	70.9±0.4	7022±162
PdAg-20	48.7±2.5	71.9±1.2	4956±193
PdAg-10	38.0±2.9	72.2±1.4	3876±92
Ag	0	0	0

[a] the values after "±" represent absolute errors.

3.2.2 H_2O_2 decomposition, hydrogenation and H_2O formation from H_2 and O_2

In order to unveil the behaviors of the catalysts in side reactions, H_2O_2 decomposition and hydrogenation were carried out in H_2O_2-methanol solutions under N_2 and H_2 atmospheres, respectively. As reported in Fig. 7, the addition of a small amount of Ag to Pd resulted in lower H_2O_2 decomposition rate and the decomposition reaction was entirely inhibited when the Pd/Ag ratio was less than 40. The H_2O_2 hydrogenation rate also decreased with the Ag added as well. The H_2O_2 hydrogenation rate of PdAg-60 (7808 mol H_2O_2 kg_{Pd}^{-1} h^{-1}) was obvious lower than the mono Pd (9854 mol H_2O_2 kg_{Pd}^{-1} h^{-1}), and it further decreased with a continuous increase of Ag content. Thus we can conclude that the addition of Ag can effectively suppress the H_2O_2 hydrogenation and decomposition reactions. It also should be noted that the conversion rate of H_2O_2 hydrogenation reaction was much larger than that of the H_2O_2 decomposition reaction.

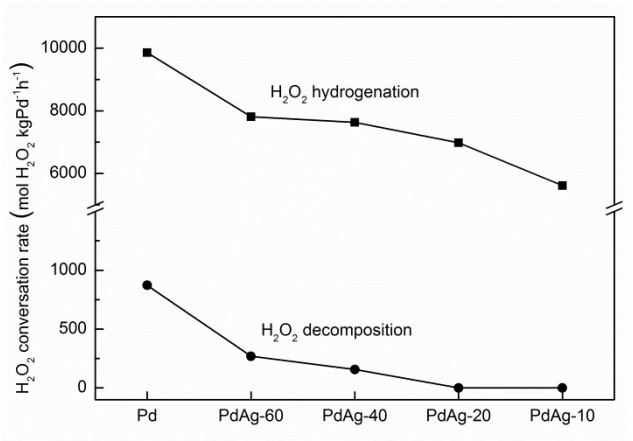

Fig. 7 Decomposition and hydrogenation of H_2O_2 over all catalysts.

We further analysis the behaviors of the catalysts in the H_2O formation from H_2 and O_2. We reduced the reaction time from 15 to 4 minutes and the amount of catalyst from 0.2 g to 0.05 g, in order to control the H_2 conversions within 10%. At very low conversion of H_2, the contribution to the overall rate of H_2O_2 synthesis from the sequential hydrogenation of H_2O_2 and the sequential decomposition of H_2O_2 both become negligible.[31] So the H_2O formation from H_2 and O_2 was the main side reaction responsible for lowering the selectivity to H_2O_2. In these experiments, the Pd/C catalyst showed a H_2 conversion of 9.0% and a H_2O_2 selectivity of 76.6%, implying that the mono Pd catalyst was also very active for the H_2O formation from H_2 and O_2. Whereas for the PdAg-40, a H_2 conversion of 5.7% and a H_2O_2 selectivity of 98.0% were obtained. Hence, the addition of Ag could effectively suppress the formation of H_2O from H_2 and O_2. Moreover, the major loss of selectivity with the PdAg catalysts was associated with the sequential hydrogenation of the H_2O_2.

4. Discussion

The addition of Ag to the Pd/C samples caused a decrease in activity but a reverse trend of selectivity for the direct synthesis of H_2O_2. It could be explained that

both ensemble effect and electronic effect existed in PdAg catalysts as the experimental results revealed.

In this study, the formation of alloys in PdAg catalysts was demonstrated by the XRD patterns, meanwhile the alloy surfaces were enriched with Ag as evidenced by XPS analysis. As a consequence, the Pd atoms in alloy surfaces were diluted with Ag, and thus led to more Pd monomer sites and less contiguous Pd ensembles existing on the surface, which have been confirmed by other researches.[47, 49-51, 54, 76] For the direct synthesis of H_2O_2, -OOH formed from the interaction of atomic H and molecular O_2 was considered to be the primary intermediate species in the generation of H_2O_2. Therefore the activation of molecularly absorbed O_2 without dissociation was vital important for this reaction system. Theoretical calculations and experimental results have evidenced that monomer Pd sites played a key role in the generation of H_2O_2 by suppressing O-O bond scission but were unfavorable for H_2O formation.[36, 77, 78] On the basis of this verdict, we could conclude that the ensemble effect that Ag reduced the number of contiguous Pd ensembles and increased Pd monomer sites effectively prevented the H_2O formation from H_2 and O_2.

For H_2O_2 decomposition and hydrogenation reactions, the addition of Ag to Pd resulted in lower H_2O_2 conversion rate. The above XPS and TPR results have proved that Ag elevated the fraction of Pd^{2+} as a result of the electronic interaction between Pd and Ag. While Pd^{2+} has been demonstrated to have a lower H_2O_2 decomposition and hydrogenation activity than corresponding Pd^0, because that H_2O_2 were more inclined to get absorbed on the Pd^0 sites.[10, 79-81] Besides that, contiguous Pd

ensembles[36] and the adsorption capability to H_2 over the catalysts also affected the H_2O_2 hydrogenation activity.

Moreover, the addition of Ag led to a drastic decrease of the H_2 conversion. It could be explained that the coverage of Ag on the Pd surface blocked the adsorption of reactants on the Pd sites, thus reduced adsorption capacity of H_2 and O_2 over these catalysts, as determined by H_2- and O_2-TPD.

It should also be noted that the PdAg alloy surfaces were enriched with Ag, which could explain why a little amount of Ag addition to Pd had such a great influence on the catalytic performance.

5. Conclusion

The performance of Pd catalysts could be improved upon alloying with Ag. A volcano-shape curve and an increased trend were observed for H_2O_2 productivity and selectivity, respectively. Among all the catalysts, PdAg-40 catalyst exhibited the best performance with a decent H_2O_2 productivity of 7022 mol kg_{Pd}^{-1} h^{-1} and a high selectivity of 70.9%.

Both ensemble effect and electronic effect detected in these PdAg catalysts resulted in the improvement of selectivity. The ensemble effect could be depicted as the addition of Ag increased monomer Pd sites and reduced contiguous Pd sites, which effectively prevented the H_2O formation from H_2 and O_2. On the other hand, the increase of Pd^{2+} caused by the electronic interaction between Pd and Ag led to a lower H_2O_2 decomposition and hydrogenation activity. That was another factor for the improved selectivity. Moreover, the decreased activity was attributed to the reduced

adsorption capacity of H_2 and O_2 due to Ag additive. These conclusions not only provide the basis for the design of novel catalysts used in the direct synthesis of H_2O_2, but also are helpful in the development of supported bimetallic PdAg catalysts for related reactions.

Acknowledgments

This work was supported by the National Natural Science Foundation of China (21106094, 21276179), the National Key Basic Research Program of China (2012CB720300) and the Program for Changjiang Scholars, Innovative Research Team in University (IRT1161).

References

1 J. M. Campos-Martin, G. Blanco-Brieva and J. L. Fierro, *Angew. Chem., Int. Ed.*, 2006, 45, 6962-6984.
2 H. Shang, H. Zhou, Z. Zhu and W. Zhang, *J. Ind. Eng. Chem.*, 2012, 18, 1851-1857.
3 J. Tan, J. S. Zhang, Y. C. Lu, J. H. Xu and G. S. Luo, *AIChE J.*, 2012, 58, 1326-1335.
4 Y. Han, Z. Y. He, S. L. Wang, W. Li and J. L. Zhang, *Catal. Sci. Technol.*, 2015, 5, 2630-2639.
5 Y. Han, Z. Y. He, Y. C. Guan, W. Li and J. L. Zhang, *Acta Phys. Chim. Sin.*, 2015, 31, 729-737.
6 J. Garc á-Serna, T. Moreno, P. Biasi, M. J. Cocero, J. P. Mikkola and T. O. Salmi, *Green Chem.*, 2014, 16, 2320.
7 A. Drelinkiewicz and A. Waksmundzka-G ára, *J. Mol. Catal. A: Chem.*, 2006, 246, 167-175.
8 R. Kosydar, A. Drelinkiewicz and J. P. Ganhy, *Catal. Lett.*, 2010, 139, 105-113.
9 T. Nishimi, T. Kamachi, K. Kato, T. Kato and K. Yoshizawa, *Eur. J. Org. Chem.*, 2011, 2011, 4113-4120.
10 C. Samanta, *Appl. Catal., A*, 2008, 350, 133-149.
11 D. Dissanayake, *J. Catal.*, 2003, 214, 113-120.
12 J. Lunsford, *J. Catal.*, 2003, 216, 455-460.
13 S. Melada, R. Rioda, F. Menegazzo, F. Pinna and G. Strukul, *J. Catal.*, 2006, 239, 422-430.
14 E. Ghedini, F. Menegazzo, M. Signoretto, M. Manzoli, F. Pinna and G. Strukul, *J. Catal.*, 2010, 273, 266-273.
15 J. Kim, Y. M. Chung, S. M. Kang, C. H. Choi, B. Y. Kim, Y. T. Kwon, T. J. Kim, S. H. Oh and C. S. Lee, *ACS Catal.*, 2012, 2, 1042-1048.

16 F. Menegazzo, M. Signoretto, G. Frison, F. Pinna, G. Strukul, M. Manzoli and F. Boccuzzi, *J. Catal.*, 2012, 290, 143-150.
17 A. Pashkova, L. Greiner, U. Krtschil, C. Hofmann and R. Zapf, *Appl. Catal., A*, 2013, 464-465, 281-287.
18 B. Z. Hu, W. P. Deng, R. S. Li, Q. H. Zhang, Y. Wang, F. Delplanque-Janssens, D. Paul, F. Desmedt and P. Miquel, *J. Catal.*, 2014, 319, 15-26.
19 L. K. Ouyang, P. F. Tian, G. J. Da, X. C. Xu, C. Ao, T. Y. Chen, R. Si, J. Xu and Y. F. Han, *J. Catal.*, 2015, 321, 70-80.
20 J. Edwards, B. Solsona, P. Landon, A. Carley, A. Herzing, C. Kiely and G. J. Hutchings, *J. Catal.*, 2005, 236, 69-79.
21 J. K. Edwards, B. Solsona, P. Landon, A. F. Carley, A. Herzing, M. Watanabe, C. J. Kiely and G. J. Hutchings, *J. Mater. Chem.*, 2005, 15, 4595.
22 J. K. Edwards, A. F. Carley, A. A. Herzing, C. J. Kiely and G. J. Hutchings, *Faraday Discuss.*, 2008, 138, 225-239.
23 J. K. Edwards and G. J. Hutchings, *Angew. Chem., Int. Ed.*, 2008, 47, 9192-9198.
24 J. K. Edwards, E. Ntainjua, A. F. Carley, A. A. Herzing, C. J. Kiely and G. J. Hutchings, *Angew. Chem., Int. Ed.*, 2009, 48, 8512-8515.
25 J. K. Edwards, B. Solsona, E. N. N, A. F. Carley, A. A. Herzing, C. J. Kiely and G. J. Hutchings, *Science*, 2009, 323, 1037-1041.
26 J. Pritchard, L. Kesavan, M. Piccinini, Q. He, R. Tiruvalam, N. Dimitratos, J. A. Lopez-Sanchez, A. F. Carley, J. K. Edwards, C. J. Kiely and G. J. Hutchings, *Langmuir*, 2010, 26, 16568-16577.
27 J. C. Pritchard, Q. He, E. N. Ntainjua, M. Piccinini, J. K. Edwards, A. A. Herzing, A. F. Carley, J. A. Moulijn, C. J. Kiely and G. J. Hutchings, *Green Chem.*, 2010, 12, 915.
28 J. K. Edwards, J. Pritchard, M. Piccinini, G. Shaw, Q. He, A. F. Carley, C. J. Kiely and G. J. Hutchings, *J. Catal.*, 2012, 292, 227-238.
29 M. Sankar, Q. He, M. Morad, J. Pritchard, S. J. Freakley, J. K. Edwards, S. H. Taylor, D. J. Morgan, A. F. Carley, D. W. Knight, C. J. Kiely and G. J. Hutchings, *ACS Nano*, 2012, 6, 6600-6613.
30 S. J. Freakley, M. Piccinini, J. K. Edwards, E. N. Ntainjua, J. A. Moulijn and G. J. Hutchings, *ACS Catal.*, 2013, 3, 487-501.
31 J. K. Edwards, S. J. Freakley, A. F. Carley, C. J. Kiely and G. J. Hutchings, *Acc. Chem. Res.*, 2014, 47, 845-854.
32 Y. F. Han, Z. Y. Zhong, K. Ramesh, F. X. Chen, L. W. Chen, T. White, Q. Tay, S. N. Yaakub and Z. Wang, *J. Phys. Chem. C*, 2007, 111, 8410-8413.
33 F. Menegazzo, P. Burti, M. Signoretto, M. Manzoli, S. Vankova, F. Boccuzzi, F. Pinna and G. Strukul, *J. Catal.*, 2008, 257, 369-381.
34 F. Menegazzo, M. Signoretto, M. Manzoli, F. Boccuzzi, G. Cruciani, F. Pinna and G. Strukul, *J. Catal.*, 2009, 268, 122-130.
35 J. K. Edwards, J. Pritchard, L. Lu, M. Piccinini, G. Shaw, A. F. Carley, D. J. Morgan, C. J. Kiely and G. J. Hutchings, *Angew. Chem., Int. Ed.*, 2014, 53, 2381-2384.
36 L. K. Ouyang, G. J. Da, P. F. Tian, T. Y. Chen, G. D. Liang, J. Xu and Y. F. Han, *J. Catal.*, 2014, 311, 129-136.
37 Q. Liu, J. C. Bauer, R. E. Schaak and J. H. Lunsford, *Appl. Catal., A*, 2008, 339, 130-136.

38 G. Bernardotto, F. Menegazzo, F. Pinna, M. Signoretto, G. Cruciani and G. Strukul, *Appl. Catal., A*, 2009, 358, 129-135.
39 J. Xu, L. Ouyang, G. J. Da, Q. Q. Song, X. J. Yang and Y. F. Han, *J. Catal.*, 2012, 285, 74-82.
40 S. Sterchele, P. Biasi, P. Centomo, P. Canton, S. Campestrini, T. Salmi and M. Zecca, *Appl. Catal., A*, 2013, 468, 160-174.
41 Q. Zhang, J. Li, X. Liu and Q. Zhu, *Appl. Catal., A*, 2000, 197, 221-228.
42 P. Praserthdam, B. Ngamsom, N. Bogdanchikova, S. Phatanasri and M. Pramotthana, *Appl. Catal., A*, 2002, 230, 41-51.
43 R. Lamb, *Appl. Catal., A*, 2004, 268, 43-50.
44 N. A. Khan, S. Shaikhutdinov and H. J. Freund, *Catal. Lett.*, 2006, 108, 159-164.
45 W. Huang, W. Pyrz, R. F. Lobo and J. G. Chen, *Appl. Catal., A*, 2007, 333, 254-263.
46 A. Pachulski, R. Schödel and P. Claus, *Appl. Catal., A*, 2012, 445-446, 107-120.
47 I. Y. Ahn, J. H. Lee, S. K. Kim and S. H. Moon, *Appl. Catal., A*, 2009, 360, 38-42.
48 A. Pachulski, R. Schödel and P. Claus, *Appl. Catal., A*, 2011, 400, 14-24.
49 H. Gu, B. L. Xu, J. Zhou, Y. Z. Li, Y. N. Fan, *Acta Phys. Chim. Sin.*, 2006, 22, 712-715.
50 D. W. Zhang, M. W. Qi and H. B. Yu, *CIESC J.*, 2011, 62, 71-77.
51 S. Hirasawa, H. Watanabe, T. Kizuka, Y. Nakagawa and K. Tomishige, *J. Catal.*, 2013, 300, 205-216.
52 S. Hirasawa, Y. Nakagawa and K. Tomishige, *Catal. Sci. Technol.*, 2012, 2, 1150.
53 A. Yarulin, I. Yuranov, F. Cárdenas-Lizana, D. T. L. Alexander and L. Kiwi-Minsker, *Appl. Catal., A*, 2014, 478, 186-193.
54 H. Zea, K. Lester, A. K. Datye, E. Rightor, R. Gulotty, W. Waterman and M. Smith, *Appl. Catal., A*, 2005, 282, 237-245.
55 S. Abate, G. Centi, S. Perathoner and F. Frusteri, *Catal. Today*, 2006, 118, 189-197.
56 S. Abate, S. Melada, G. Centi, S. Perathoner, F. Pinna and G. Strukul, *Catal. Today*, 2006, 117, 193-198.
57 L. Wang, S. Bao, J. Yi, F. He and Z. Mi, *Appl. Catal., B*, 2008, 79, 157-162.
58 C. A. Farberow, A. Godinez-Garcia, G. Peng, J. F. Perez-Robles, O. Solorza-Feria and M. Mavrikakis, *ACS Catal.*, 2013, 3, 1622-1632.
59 P. Kittisakmontree, B. Pongthawornsakun, H. Yoshida, S. I. Fujita, M. Arai and J. Panpranot, *J. Catal.*, 2013, 297, 155-164.
60 S. T. Nguyen, H. M. Law, H. T. Nguyen, N. Kristian, S. Wang, S. H. Chan and X. Wang, *Appl. Catal., B*, 2009, 91, 507-515.
61 W. J. Zhou, W. Z. Li, S. Q. Song, Z. H. Zhou, L. H. Jiang, G. Q. Sun, Q. Xin, K. Poulianitis, S. Kontou and P. Tsiakaras, *J. Power Sources*, 2004, 131, 217-223.
62 G. Zhang, Y. Wang, X. Wang, Y. Chen, Y. Zhou, Y. Tang, L. Lu, J. Bao and T. Lu, *Appl. Catal., B*, 2011, 102, 614-619.
63 B. Ngamsom, *Catal. Commun.*, 2004, 5, 243-248.
64 W. Tiano, M. Dapiaggi and G. Artioli, *J. Appl. Cryst.*, 2003, 36, 1461-1463.
65 J. T. Feng, H. Y. Wang, D. G. Evans, X. Duan and D. Q. Li, *Appl. Catal., A*, 2010, 382, 240-245.
66 S. Karski, I. Witonska, J. Rogowski and J. Goluchowska, *J. Mol. Catal. A: Chem.*, 2005, 240, 155-163.
67 G. Fagherazzi, A. Benedetti, S. Polizzi, A. Di Mario, F. Pinna, M. Signoretto and N. Pernicone,

Catal. Lett., 1995, 32, 293-303.
68 X. Yang, D. Chen, S. Liao, H. Song, Y. Li, Z. Fu and Y. Su, *J. Catal.*, 2012, 291, 36-43.
69 Y. Y. Feng, Z. H. Liu, W. Q. Kong, Q. Y. Yin and L. X. Du, *Int. J. Hydrogen Energ.*, 2014, 39, 2497-2504.
70 Practical Surface Analysis, Auger and X-ray Photoelectron Spectroscopy, ed. D. Briggs and M. P. Seah, New York: Wiley; Volume 1: 2nd edn.1990.
71 E. G. Allison and G. C. Bond, *Catal. Rev.*, 2006, 7, 233-289.
72 A. M. Venezia, L. F. Liotta, G. Deganello, Z. Schay and L. Guczi, *J. Catal.*, 1999, 182, 449-455.
73 P. J. Berlowitz and D. W. Goodman, *Langmuir*, 1988, 4, 1091-1095.
74 C. E. G. Vfctor and H. Sandoval, *Appl. Catal., A*, 1996, 148, 81-96.
75 C. Amorim and M. A. Keane, *J. Colloid Interf. Sci.*, 2008, 322, 196-208.
76 Y. Soma-noto and W. M. H. Sachtler, *J. Catal.*, 1974, 32, 315-324.
77 H. C. Ham, G. S. Hwang, J. Han, S. W. Nam and T. H. Lim, *J. Phys. Chem. C*, 2009, 113, 12943-12945.
78 D. W. Yuan, Z. R. Liu and Y. Xu, *Phys. Lett. A*, 2012, 376, 3432-3438.
79 C. Samanta and V. R. Choudhary, *Appl. Catal., A*, 2007, 326, 28-36.
80 C. Samanta and V. R. Choudhary, *Appl. Catal., A*, 2007, 330, 23-32.
81 C. Samanta and V. R. Choudhary, *Chem. Eng. J.*, 2008, 136, 126-132.

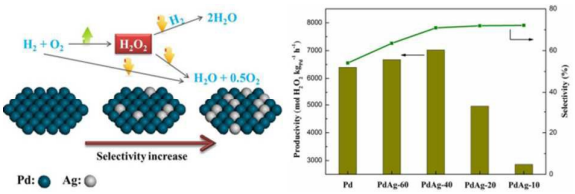

The addition of Ag to the Pd caused an increase in selectivity due to the ensemble effect and electronic effect.